

Video Article

Integration of Light Trapping Silver Nanostructures in Hydrogenated Microcrystalline Silicon Solar Cells by Transfer Printing

Hidehori Mizuno¹, Hitoshi Sai², Koji Matsubara², Hidetaka Takato¹, Michio Kondo¹

¹Renewable Energy Research Center, Fukushima Renewable Energy Institute, National Institute of Advanced Industrial Science and Technology, Koriyama, Fukushima, Japan

²Research Center for Photovoltaic Technologies, National Institute of Advanced Industrial Science and Technology, Tsukuba, Ibaraki, Japan

Correspondence to: Hidehori Mizuno at h-mizuno@aist.go.jp

URL: <https://www.jove.com/video/53276>

DOI: [doi:10.3791/53276](https://doi.org/10.3791/53276)

Keywords: Engineering, Issue 105, Transfer print, Nanofabrication, Stamp, Poly(dimethylsiloxane), Silver, Plasmon, Light trapping, Solar cell, Silicon

Date Published: 11/9/2015

Citation: Mizuno, H., Sai, H., Matsubara, K., Takato, H., Kondo, M. Integration of Light Trapping Silver Nanostructures in Hydrogenated Microcrystalline Silicon Solar Cells by Transfer Printing. *J. Vis. Exp.* (105), e53276, doi:10.3791/53276 (2015).

Abstract

One of the potential applications of metal nanostructures is light trapping in solar cells, where unique optical properties of nanosized metals, commonly known as plasmonic effects, play an important role. Research in this field has, however, been impeded owing to the difficulty of fabricating devices containing the desired functional metal nanostructures. In order to provide a viable strategy to this issue, we herein show a transfer printing-based approach that allows the quick and low-cost integration of designed metal nanostructures with a variety of device architectures, including solar cells. Nanopillar poly(dimethylsiloxane) (PDMS) stamps were fabricated from a commercially available nanohole plastic film as a master mold. On this nanopatterned PDMS stamps, Ag films were deposited, which were then transfer-printed onto block copolymer (binding layer)-coated hydrogenated microcrystalline Si ($\mu\text{-Si:H}$) surface to afford ordered Ag nanodisk structures. It was confirmed that the resulting Ag nanodisk-incorporated $\mu\text{-Si:H}$ solar cells show higher performances compared to a cell without the transfer-printed Ag nanodisks, thanks to plasmonic light trapping effect derived from the Ag nanodisks. Because of the simplicity and versatility, further device application would also be feasible through this approach.

Video Link

The video component of this article can be found at <https://www.jove.com/video/53276/>

Introduction

There has been a long-standing demand for the application of functional nanostructures in a broad range of technological field. One of the expectations for this trend is to open new design of device architectures leading to improved or innovative performances. In the field of solar cells, for example, the use of metal nanostructures has been actively explored because of their intriguing optical (*i.e.*, plasmonic) properties,¹ potentially beneficial to construct effective light trapping systems.^{2,3} Indeed, some theoretical studies⁴⁻⁶ have suggested that such plasmonic light trapping could achieve effects exceeding the conventional ray optics (texturing)-based light trapping limit.⁷ As a result, developing strategies to integrate desired metal nanostructures with solar cells has become increasingly important in order to realize these theoretical predictions.

A number of strategies have been proposed to meet this challenge.⁸⁻²⁴ These include, for instance, simple (low-cost) thermal annealing of metal films^{8,9} or dispersion of pre-synthesized metal nanoparticles,^{10,11} both of which resulted in successful demonstrations of plasmonic light trapping. However, it should be pointed out that the metal nanostructures fabricated by these approaches are usually challenging to match to the theoretical models. In contrast, the traditional nanofabrication techniques in semiconductor industries, such as photolithography and electron beam lithography,^{12,13} can control structures well below the sub-100 nm level, but they are often too expensive and time-consuming to apply to solar cells, where large-area capability with low cost is essential. In order to fulfill the low-cost, high-throughput, and large-area requirements with nanoscale controllability, methods such as nanoimprint lithography,¹⁴⁻¹⁶ soft lithography,^{17,18} nanosphere lithography,¹⁹⁻²¹ and hole-mask colloidal lithography²²⁻²⁴ would be promising. Among these choices, we have developed a soft lithographic, advanced transfer printing technique.²⁵ Using a nanostructured poly(dimethylsiloxane) (PDMS) stamps and block copolymer-based adhesive layers, patterning of ordered metal nanostructures could be readily achieved on a number of technologically relevant materials, including the ones for solar cells.

The focus of this article is to describe the detailed procedure of our transfer printing approach to incorporate effective light trapping plasmonic nanostructures in existing solar cell structures. As a demonstrative case, Ag nanodisks and thin-film hydrogenated microcrystalline Si ($\mu\text{-Si:H}$) solar cells were selected in this study (**Figure 1**),²⁶ although other types of metals and solar cells are compatible with this approach. Together with its process simplicity, the approach would be of interest to diverse researchers as a handy tool to integrate functional metal nanostructures with devices.

Protocol

1. Preparation of PDMS Stamps

1. Set a nanohole mold (nanoimprinted cyclo olefin polymer plastic film, size: 50 mm × 50 mm) in a polytetrafluoroethylene (PTFE) container.
2. Weigh vinylmethylsiloxane-dimethylsiloxane copolymer (0.76 g for the 50 mm × 50 mm mold) in a disposable glass bottle and mix it with Pt-divinyltetramethyldisiloxane complex (6 μ l, using a digital micro pipette with a disposable polypropylene tip) and 2,4,6,8-tetramethyltetra-vinylcyclotetrasiloxane (24 μ l, using a digital micro pipette with a disposable polypropylene tip).
3. Add methylhydrosiloxane-dimethylsiloxane copolymer (0.24 ml, using a digital micro pipette with a disposable polypropylene tip) in the glass bottle and mix it quickly using a disposable glass pipette. After the surface of the mold set in the PTFE container is blown by N₂, pour the resulting mixture ("hard" PDMS prepolymer) on the mold and start spin-coating at 1,000 rpm for 40 sec to achieve the layer thickness of ~40 μ m.
4. Place the spin-coated sample in a hot chamber preheated at 65 °C for 30 min to briefly cross-link the hard PDMS.
5. During the heating, weigh silicone (6 g) and mix it with catalyst (0.6 g) in a disposable glass bottle. Place the glass bottle in a vacuum desiccator and apply vacuum (~133 Pa) for 15 min to remove the air trapped in the silicone mixture ("soft" PDMS prepolymer).
6. Take out the mold and soft PDMS prepolymer from the heating chamber and vacuum desiccator, respectively, and quickly pour the soft PDMS prepolymer onto the heated mold. The thickness of soft PDMS layer is ~3 mm.
7. Place the resulting sample in the vacuum desiccator again for further degassing at ~133 Pa at least for 1 hr.
8. Transfer the degassed sample to the heating chamber and start heating gradually up to 80 °C (heating rate ~3 °C/min). Keep this temperature for 5 hr to cross-link the hard and soft PDMS completely.
9. After cooling the sample down to RT, peel off the PDMS stamp carefully from the mold. Reuse the mold to prepare the second (or more) stamps, if necessary. Note: The same mold can be used at least five times without degradation of the stamp quality.
10. Cut the resulting nanopillar stamp (double-layered hard/soft PDMS composite)²⁷ into pieces of desired sizes (typically 7 mm × 7 mm for our solar cells) using a knife and store them under air until use.

2. Preparation of Block Copolymer Solutions

1. Weigh the powder of polystyrene-*block*-poly-2-vinylpyridine (PS-*b*-P2VP) in a glass bottle and mix it with *o*-xylene in the ratio of 3 mg/ml (PS-*b*-P2VP/*o*-xylene).
2. Stir the mixture using a PTFE-coated magnetic stirring bar at 70 °C for 1 hr.
3. Keep the resulting solution for more than 24 h at RT without stirring to complete the formation of self-assembled micelles. Tightly seal the solution and store it under ambient conditions. Note: The quality of the solution is unchanged even one year after preparation.

3. Preparation of μ C-Si:H Substrates

1. Wash glasses covered with SnO₂:F (denote glass/SnO₂:F, hereafter) with H₂O (500 ml), detergent (500 ml), and H₂O (500 ml) at RT using an ultrasonic bath (15 min for each). Dry them by blowing N₂.
2. Load the cleaned glass/SnO₂:F substrates in a substrate holder and deposit ZnO:Ga (20 nm) using a direct current (DC) sputtering system with the conditions specified in **Table 2**.
3. Load the glass/SnO₂:F/ZnO:Ga substrates in another substrate holder and deposit μ C-Si:H *p* (10 nm), *i* (500 nm), and *n* (40 nm) layers using a plasma-enhanced chemical vapor deposition (PECVD) system with the conditions specified in **Table 2**.
4. Store the resulting μ C-Si:H (glass/SnO₂:F/ZnO:Ga/ μ C-Si:H *p-i-n*) substrates under vacuum or N₂ until the transfer-printing step.

4. Ag-coating of PDMS Stamps

1. Wash the PDMS stamps (prepared in step 1) with EtOH (30 ml) using an ultrasonic bath for 15 min and dry by blowing N₂.
2. Load the cleaned PDMS stamps on a sample holder using double-sided adhesive tape and deposit an Ag film (10-80 nm) using an electron beam (EB) evaporation system with following conditions: deposition rate = 5-10 Å/sec, pressure = ~1.5 × 10⁻⁴ Pa.
3. Take out the Ag-coated stamps from the EB evaporation system and use them immediately in the following transfer printing step.

5. Transfer Printing of Ag Nanodisks on Thin-film Si Surfaces

1. Take out the thin-film Si substrates stored under vacuum or N₂ and spin-coat with the PS-*b*-P2VP solution (0.3 ml for 50 mm × 50 mm sample, using a digital micro pipette with a disposable polypropylene tip) at 5,000 rpm for 40 sec.
2. Wet the PS-*b*-P2VP-coated surface with EtOH using a digital micro pipette (5 μ m/cell area) and apply the Ag-coated PDMS stamp softly to the EtOH-wet surface. Do not press the stamp.
3. Place the thin-film Si substrate with the stamp in a vacuum chamber and apply vacuum (~133 Pa).
4. After 5 min, fill the vacuum chamber with air and take out the thin-film Si substrate.
5. Remove the stamp from the thin-film Si substrate by holding the both side of the stamp with tweezers to transfer-print Ag nanodisks. Note: If successful, the trace of stamping is visible as a greenish spot.
6. Rinse the transfer-printed thin-film Si substrate with a continuous flow of EtOH for 15 sec (~30 ml) and dry by blowing N₂.
7. Remove the PS-*b*-P2VP coating using an Ar plasma system.
 1. Place the transfer-printed thin-film Si substrate in the process chamber of the Ar plasma system.
 2. Pump out the air in the process chamber for ~5 min (pressure ~20 Pa).
 3. Open the valve of an Ar gas line and manually adjust the flow rate to 4 sccm. Wait for ~5 min to stabilize the pressure to 40 Pa.

4. Generate Ar plasma for 108 sec.
5. Close the valve of the Ar gas line, stop pumping, and fill air into the process chamber to take out the plasma-cleaned, transfer-printed thin-film Si substrates.

6. Completion of Thin-film Si Solar Cell Fabrication

1. Attach metal masks to the transfer-printed thin-film Si substrates after the Ar plasma treatment using polyimide tapes.
2. Load the masked substrates in a substrate holder of a DC sputtering system and deposit ZnO:Ga (100 nm), Ag (250 nm), and ZnO:Ga (40 nm) sequentially with the conditions specified in **Table 2**.
3. Detach the metal masks from the substrates and remove the masked thin-film Si layers (*i.e.*, the area where ZnO:Ga and Ag were not deposited) using a reactive ion etching (RIE) system.
 1. Place the samples in the process chamber of the RIE system.
 2. Pump out the air in the process chamber following manufacturer's instructions.
 3. Set the process conditions as follows following the manufacturer's instruction: SF₆/O₂ flow rate = 100/20 sccm, pressure = 20 Pa, power 100 W, time = 1 min 20 sec.
 4. Open the SF₆ and O₂ gas lines, stabilize the pressure, and generate plasma.
 5. Close the valve of the SF₆ and O₂ gas line, stop pumping, and fill N₂ into the process chamber to take out the samples.
4. Put the samples in a vacuum-annealing chamber and start heating gradually up to 175 °C under vacuum (~133 Pa). Keep this temperature for 2 hr, and then allow to cool to RT. Fill air in the chamber and take out samples, which now can be called cells.
5. Solder Sn-Zn-based alloy on the front transparent electrode (glass/SnO₂:F/ZnO:Ga, the exposed part by the RIE treatment) using an ultrasonic soldering device.

7. Measurement of External Quantum Efficiency (EQE)

1. Attach a light-shielding mask to a fabricated cell using polyimide tape and set the masked cell in a cell holder. Connect probes to the front soldered electrode (+) and back Ag/ZnO:Ga electrode (-).
2. Measure EQE spectra using an EQE measurement system following manufacturer's instructions with a wavelength range and step of 300-1,100 nm and 5 nm, respectively.

8. Measurement of Photovoltaic Current-Voltage (J-V) Characteristics

1. Calibrate the light intensity of a J-V characteristics measurement system using an amorphous Si reference cell.
 1. Set the amorphous Si reference cell to a cell holder of the J-V characteristics measurement system, and illuminate the light.
 2. Read the photogenerated current using a digital multi-meter equipped in the J-V characteristics measurement system. Adjust the light intensity until the photogenerated current shows the right value for the reference cell (8.34 mA/cm²).
2. Attach a light-shielding mask to a cell and set the masked cell in a cell holder. Connect probes to the front soldered electrode (+) and back Ag/ZnO:Ga electrode (-).
3. Illuminate the calibrated light (100 mW/cm², 1 sun) on the cell and measure photogenerated currents using the J-V characteristics measurement system following manufacturer's instructions with a voltage step of 0.02 V.

Representative Results

Figure 2 outlines the general process for the transfer printing of Ag nanodisks on the surface of μ c-Si:H (*n* layer). Briefly, an Ag film (thickness: 10-80 nm) is first deposited on the surface of a nanopillar PDMS stamp by electron beam evaporation. In parallel, a PS-*b*-P2VP solution is spin-coated on the surface of a freshly prepared μ c-Si:H *n* layer. Subsequently, a droplet of EtOH is placed on the PS-*b*-P2VP-coated surface, and the Ag-deposited PDMS stamp is placed on the EtOH-wet PS-*b*-P2VP surface. No pressing is necessary to the stamp, because an intimate contact between the stamp and substrate spontaneously forms due to the surface tension derived from the evaporation of the EtOH. After the EtOH is evaporated away (using a reduced pressure), the stamp is released from the substrate to complete the transfer of the Ag deposited on the raised region of the nanopillar PDMS stamp. Finally, an Ar plasma treatment is carried out to remove the PS-*b*-P2VP coating.

Shown in **Figure 3** are scanning electron microscopy (SEM) images of the resulting Ag nanodisk array on (in) μ c-Si:H surfaces (cells).²⁶ **Figure 3A** and **3B** are the top and tilted views of a same sample. The root mean square roughness (R_{rms}) of the underlying μ c-Si:H surface was 6.6 nm; nevertheless, nearly complete transfer of the Ag nanodisks, whose diameter, center-to-center distance, and the thickness of the Ag nanodisks were 200, 460, and 40 nm, respectively, was achieved. **Figure 3C** is the cross-sectional view of a completed μ c-Si:H cell structure; *i.e.*, after the deposition (sputtering) of ZnO:Ga/Ag/ZnO:Ga layers on top of the Ag nanodisk array shown in **Figure 3A** and **3B**. The embedded Ag nanodisks right on the photovoltaic μ c-Si:H *p-i-n* layers were clearly observed.

The EQE spectra of the fabricated cells are shown in **Figure 4**.²⁶ Compared to a reference cell (a μ c-Si:H cell fabricated simultaneously with skipping the transfer printing process), the EQE spectrum of the Ag nanodisk (thickness: 40 nm) incorporated cell showed higher signals in the long wavelength range (650-1,100 nm). Such wavelength-selective enhancement clearly indicated the preferential effect of the plasmonically-active Ag nanodisks for solar cell; namely, plasmonic light trapping. Quantification of the degree of the light trapping in the 650-1,100 nm range observed in **Figure 3** was carried out by summing the EQE values of each cell and taking the ratio of them (Ag nanodisk-incorporated cell/reference cell). The value was 1.60; therefore, 60% EQE increase was achieved by the Ag nanodisk-mediated plasmonic light trapping.

Table 1 summarizes the photovoltaic characteristics of the Ag nanodisk-incorporated and reference cells.²⁶ It was confirmed, as expected, that the short-circuit current density (J_{sc}) of the Ag nanodisk-incorporated cell increased compared to that of the reference cell (11.4 to 12.4 mA/cm²) because of the EQE enhancement described above. As for the open-circuit voltage (V_{oc}) and fill factor (FF), those of the two cells were almost the same (V_{oc} : ~0.52 V, FF: ~0.76). As a consequence, the photoconversion efficiency (η) of the Ag nanodisk-incorporated cell improved (4.5% to 5.0%).

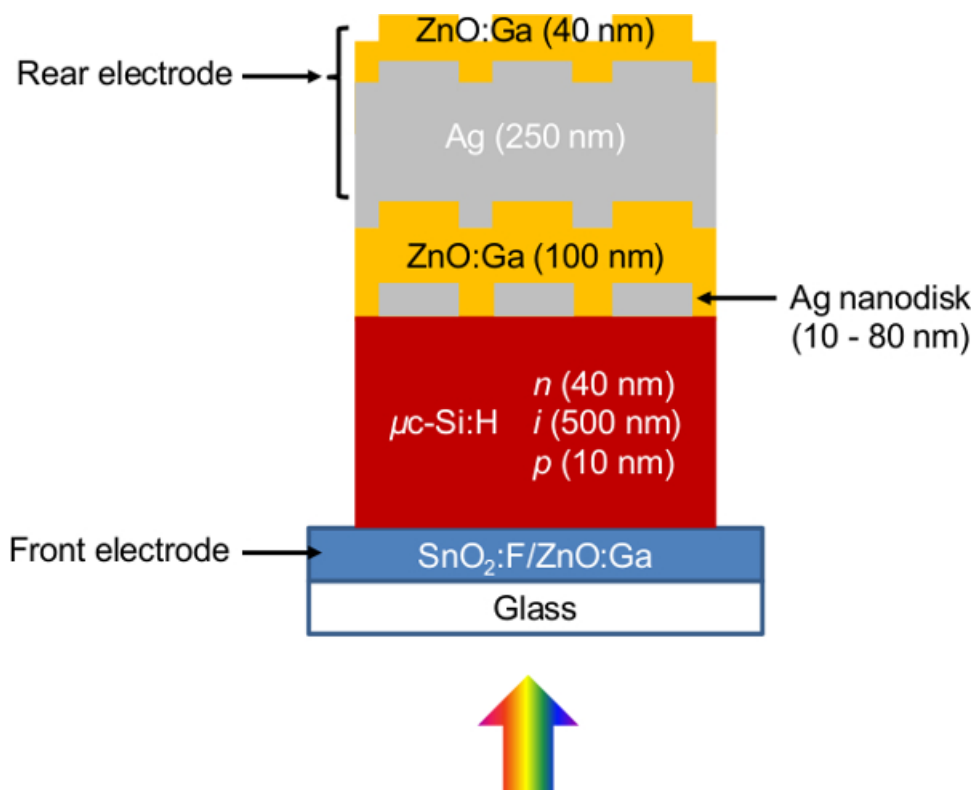


Figure 1. Schematic Cross-Section of a Ag nanodisk-incorporated μ c-Si:H solar cell. The Ag nanodisks locate at the rear side of the μ c-Si:H solar cell. [Please click here to view a larger version of this figure.](#)

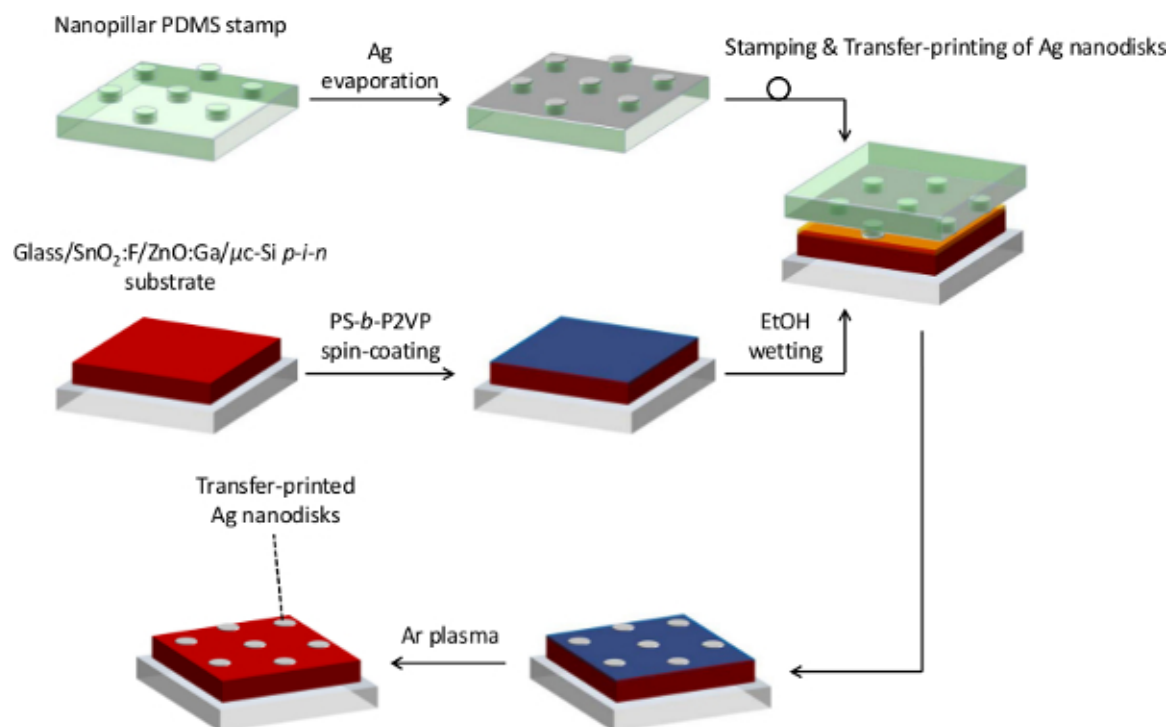


Figure 2. General Procedure for the Transfer printing of Ag Nanodisks. The Ag-coated nanopillar PDMS stamp is applied onto the PS-*b*-P2VP-coated thin-film Si substrate whose surface is wet with EtOH. Ar plasma treatment is applied to remove the PS-*b*-P2VP coating and to expose the thin-film Si layer. After this process, ZnO:Ga/Ag/ZnO:Ga layers need to be deposited on top of the transfer-printed Ag nanodisks to complete the entire solar cell structure shown in **Figure 1**. [Please click here to view a larger version of this figure.](#)

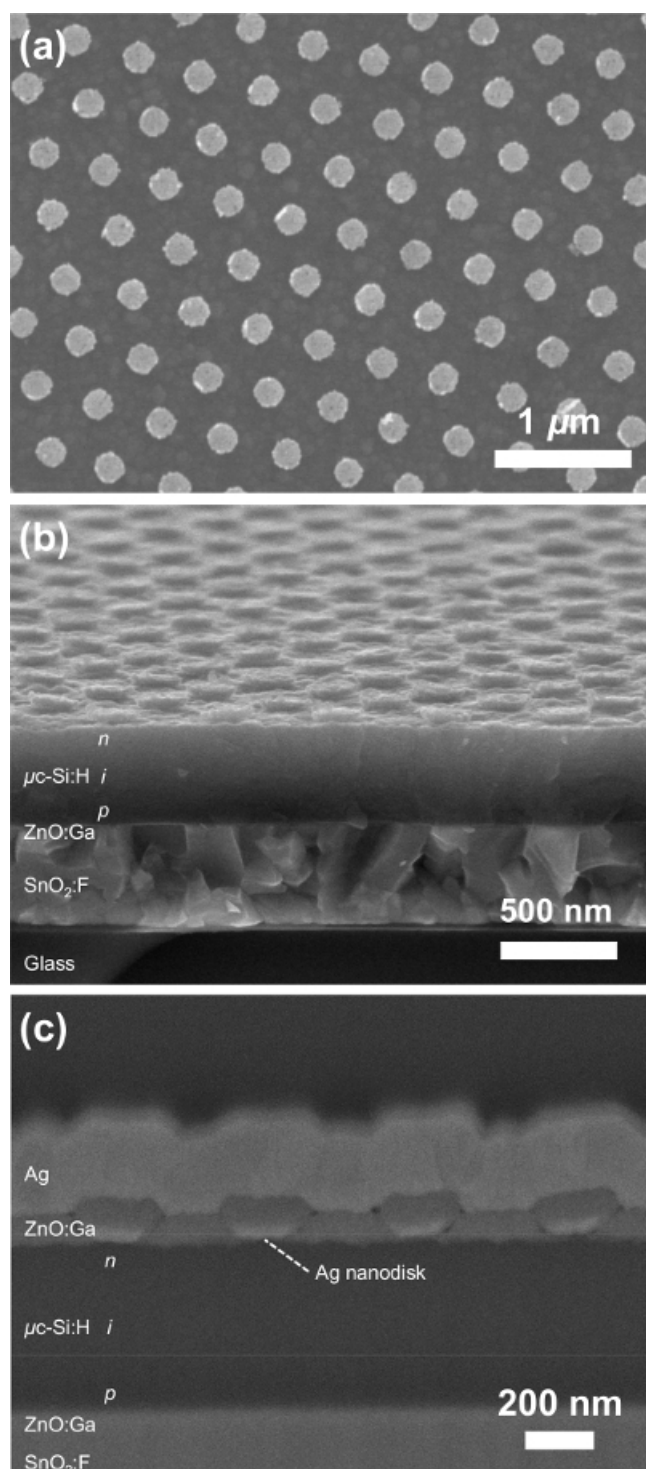


Figure 3. SEM Images of Transfer-Printed Ag Nanodisks (diameter = 200 nm, thickness = 40 nm). (A) Top view of transfer-printed Ag nanodisks on a $\mu\text{c-Si:H}$ surface. (B) Tilted view of transfer-printed Ag nanodisks on a $\mu\text{c-Si:H}$ surface. (C) Cross-sectional view of transfer-printed Ag nanodisks (size: 200 nm) embedded in a $\mu\text{c-Si:H}$ cell.²⁶ Copyright 2014 The Japan Society of Applied Physics. [Please click here to view a larger version of this figure.](#)

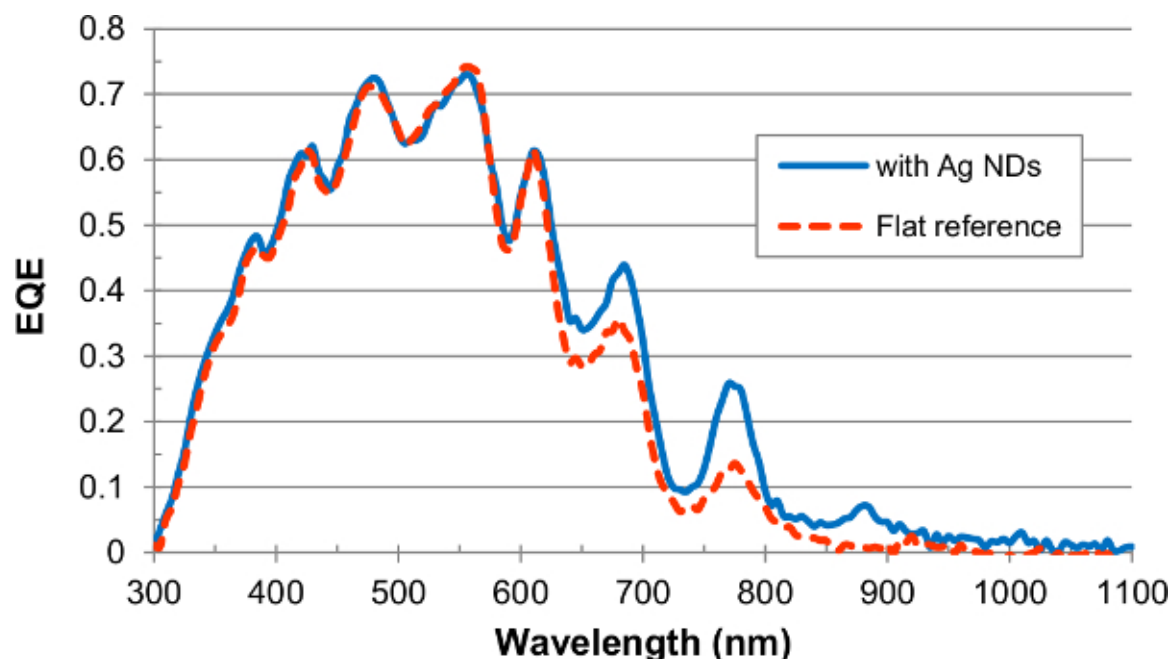


Figure 4. EQE Spectra of $\mu\text{c-Si:H}$ cells. (Blue line) Ag nanodisk (ND)-incorporated cell. (Red dashed line) Reference cell.²⁶ Improved responses were observed with the blue line owing to the Ag ND-mediated light trapping. This figure has been modified from Ref. 26. [Please click here to view a larger version of this figure.](#)

Table 1. Summary of Photovoltaic J-V Characteristics of $\mu\text{c-Si:H}$ cells.

Cell type	J_{sc} (mA/cm ²)	V_{oc} (V)	FF	η (%)
Ag nanodisk-incorporated	12.4	0.526	0.764	5
Reference	11.4	0.521	0.763	4.5

Table 2. Deposition conditions.

Steps	Deposition system	Materials	Conditions
3.2	Sputtering	ZnO:Ga	Ar flow rate = 200 sccm, pressure = 0.133 Pa, DC power = 200 W, sample rotation = 10 rpm, deposition rate = ~3.3 Å/sec.
3.3	CVD	$\mu\text{c-Si:H p}$	Flow rate of $\text{SiH}_4/\text{H}_2/\text{B}_2\text{H}_6$ = 3.5/450/2 sccm, substrate temperature = 140 °C, pressure = 1.5 torr, radio frequency (RF) power density = 80 mW/cm ² , deposition time = 5 min 45 sec (rate = ~0.3 Å/sec).
		$\mu\text{c-Si:H i}$	Flow rate of SiH_4/H_2 = 10.5/380 sccm, substrate temperature = 180 °C, pressure = 200 Pa, RF power density = 40 mW/cm ² , deposition time = 1 hr 2 min (rate = ~1.3 Å/sec).
		$\mu\text{c-Si:H n}$	Flow rate of $\text{SiH}_4/\text{H}_2/\text{PH}_3$ = 3/148/12 sccm, substrate temperature = 195 °C, pressure = 40 Pa, RF power density = 80 mW/cm ² , deposition time = 23 min (rate = ~0.3 Å/sec).

6.2	Sputtering	ZnO:Ga	Ar flow = 200 sccm, pressure = 0.133 Pa, DC power = 200 W, sample rotation = 10 rpm, deposition rate = ~3.3 Å/sec.
		Ag	Ar flow = 200 sccm, pressure = 0.133 Pa, DC power = 100 W, sample rotation = 10 rpm, deposition rate = ~6 Å/sec.

Discussion

In this article, a double-layered hard/soft PDMS composite was employed as stamp materials.²⁷ This combination was found to be essential to precisely replicate the parent nanostructure in the mold, which was a hexagonally close-packed round-hole array whose diameter of 230 nm, depth of 500 nm, and hole center-to-center spacing of 460 nm. When only soft PDMS was used, the stamp always resulted in a poorly nanostructured surface (for example, no sharp edge in the inverted pillar structure) due to the low Young's modulus,²⁸ therefore, transfer printing of Ag nanodisks was never achievable.

The use of spin-coated block copolymer (PS-*b*-P2VP) thin-films as binding layers is another key for successful transfer printing on the μ c-Si:H surfaces, which are not smooth (R_{rms} = ~6.6 nm). Although the transfer-printing of metal structures was originally developed using small organic molecules which forms self-assembled monolayers (SAMs) on surfaces,²⁹ we found that the use of SAMs (3-mercaptopropyltrimethoxysilane) does not work for the (slightly) textured μ c-Si:H surfaces. In addition, the formation of SAMs with good quality takes time (~a couple of hours), while our process requires less than 1 min (40 sec by spin coating). This point might be important for materials which need quick operations to avoid unfavorable surface events, such as the formation of excess oxides or contaminations.

The roles of EtOH in transfer printing should also be emphasized. The first role is, as already described, to assist the formation of the intimate contact between the stamp and target surface using the surface tension upon evaporation. The second role is to reconstruct the PS-*b*-P2VP thin film, which ensures the capturing of metals (Ag) on PDMS stamps through the formation of metal-pyridine coordination bonds.²⁵ We believe that such dynamic event at the stamp/substrate interface is essential for the transfer printing especially on textured surfaces.

When the transfer printing by above procedure was unsuccessful, the reason was mostly in stamps employed. Since conformal contact between a stamp and a substrate is critical, the flatness of the stamp's surface is very important. The flatness is determined by the status of an original mold; therefore, once transfer printing fails, it would be the time for changing the mold. According to our experience, the number of times a mold can be reused is five, but it would be increased by appropriate cleaning and storing of the mold. Flatness of a stamp would also have a significant impact on the area that can be uniformly transfer-printed. In this regards, we have demonstrated a 20 mm × 20 mm-scale patterning with a stamp prepared from a fresh mold.²⁵

As for the pattern design of the mold/stamp, round-hole/pillar structures with the diameter of 230/200 nm were employed (the smaller diameter of the pillar is due to the tapered shape of the original hole). This choice was simply because such a mold (nanoimprinted plastic film) was commercially available, and it was not the one fabricated specifically to our solar cell application. This in turn means that there is plenty of room for pattern designs, which would lead to much superior light trapping ability compared to the result shown here. In this respect, the use of optical simulation would be helpful to search better patterns. Although the fabrication of actual molds (probably by electron beam lithography) can be expensive, once fabricated, the corresponding stamps can be replicated as many times as needed. Thus, the total process cost can be significantly suppressed, which is the great advantage of transfer printing approaches.

In terms of the metals transfer-printable by the procedure described here, Au, Cu, and Ni were confirmed to be applicable. It should be mentioned that none of these metals provided better light trapping effects compared to the case of Ag. Another metal tested was Al, which is considered as a good candidate for plasmonic light trapping applications.³⁰ It was found, however, that transfer printing of Al is unsuccessful, possibly due to the strong affinity with PDMS. Therefore, modifications of PDMS surfaces³¹ may be required to facilitate transfer printing by reducing the interaction between PDMS and deposited Al.

Other than μ c-Si:H, the method can be used with a variety of materials, including highly rough (textured) surfaces (R_{rms} ≥ 20 nm).²⁵ In fact, we have previously addressed the possibility of synergistic texturing/plasmon-mediated light trapping by fabricating cells with textured glass/SnO₂:F substrates.¹⁷ In addition, a similar light trapping effect has been documented using hydrogenated amorphous Si cells.³² Other technologically important materials, such as crystalline Si, GaAs, InP, and metal oxides, are also compatible with the method, and thus further device applications (not only for solar cells) would be expected.

Disclosures

The authors have nothing to disclose.

Acknowledgements

The authors thank New Energy and Industrial Technology Development Organization (NEDO) under Ministry of Economy, Trade, and Industry (METI), Japan, for the financial support.

References

1. Murray, W.A., Barnes, W.L. Plasmonic Materials. *Adv. Mater.* **19**, 3771-3782, (2007).
2. Atwater, H.A., Polman, A. Plasmonics for improved photovoltaic devices. *Nat. Mater.* **9**, 205-213, (2010).
3. Green, M. A., Pillai, S. Harnessing plasmonics for solar cells. *Nat. Photon.* **6**, 130-132, (2012).
4. Yu, Z., Raman, A., Fan, S. Fundamental limit of nanophotonic light trapping in solar cells. *Proc. Natl. Acad. Sci. U.S.A.* **107**, 17491-17496, (2010).
5. Callahan, D. M., Munday, J. N., Atwater, H. A. Solar Cell Light Trapping beyond the Ray Optic Limit. *Nano Lett.* **12**, 214-218, (2012).
6. Biswas, R., Xu, C. Photonic and plasmonic crystal based enhancement of solar cells-Theory of overcoming the Lambertian limit. *J. Non-Cryst. Solids* **358**, 2289-2294, (2012).
7. Yablonovitch, E. Statistical ray optics. *J. Opt. Soc. Am.* **72**, 899-907, (1982).
8. Chantana, J., et al. Localized surface plasmon enhanced microcrystalline silicon solar cells. *J. Non-Cryst. Solids* **358**, 2319-2323, (2012).
9. Tan, H., Santbergen, R., Smets, A. H. M., Zeman, M. Plasmonic Light Trapping in Thin-film Silicon Solar Cells with Improved Self-Assembled Silver Nanoparticles. *Nano Lett.* **12**, 4070-4076, (2012).
10. Mizuno, H., Sai, H., Matsubara, K., Kondo, M. Light Trapping by Ag Nanoparticles Chemically Assembled inside Thin-Film Hydrogenated Microcrystalline Si Solar Cells. *Jpn. J. Appl. Phys.* **51**, 042302-1-4, (2012).
11. Chen, X., et al. Broadband Enhancement in Thin-Film Amorphous Silicon Solar Cells Enabled by Nucleated Silver Nanoparticles. *Nano Lett.* **12**, 2187-2192, (2012).
12. Spinelli, P., et al. Optical Impedance Matching Using Coupled Plasmonic Nanoparticle Arrays. *Nano Lett.* **11**, 1760-1765, (2011).
13. Temple, T. L., Bagnall, D. M. Optical properties of gold and aluminium nanoparticles for silicon solar cell applications. *J Appl. Phys.* **109**, 084343-1-13, (2011).
14. Ferry, V. E., et al. Optimized Spatial Correlations for Broadband Light Trapping Nanopatterns in High Efficiency Ultrathin Film a-Si:H Solar Cells. *Nano Lett.* **11**, 4239-4245, (2011).
15. Paetzold, U. W., et al., Plasmonic reflection grating back contacts for microcrystalline silicon solar cells. *Appl. Phys. Lett.* **99**, 181105-1-3, (2011).
16. Chou, S. Y., Krauss, P.R., Renstrom, P. J. Nanoimprint Lithography, *J. Vac. Sci. Technol. B.* **14**, 4129 - 4133, (1996).
17. Na, S.-I., et al. Efficient Polymer Solar Cells with Surface Relief Gratings Fabricated by Simple Soft Lithography. *Adv. Funct. Mater.* **18**, 3956 - 3963, (2008).
18. Xia, Y., Whitesides, G. M. Soft Lithography. *Angew. Chem. Int. Ed.* **37**, 550 - 575, (1998).
19. Battaglia, C., et al., Light Trapping in Solar Cells: Can Periodic Beat Random? *ACS Nano* **6**, 2790-2797, (2012).
20. Hsu, C.-M., et al., High-Efficiency Amorphous Silicon Solar Cell on a Periodic Nanocone BackReflector. *Adv. Energy Mater.* **2**, 628-633, (2012).
21. Hulst, J. C., Van Duyne, R. P., Nanosphere lithography: A materials general fabrication process for periodic particle array surfaces. *J. Vac. Sci. Technol. A.* **13**, 1553-1558, (1995).
22. Daif, O. E., et al., Front side plasmonic effect on thin silicon epitaxial solar cells. *Sol. Energy Mater. Sol. Cells* **104**, 58-63, (2012).
23. Niesen, B. et al., Plasmonic Efficiency Enhancement of High Performance Organic Solar Cells with a Nanostructured Rear Electrode. *Adv. Energy Mater.* **3**, 145-150, (2013).
24. Fredriksson, H., et al., Hole-Mask Colloidal Lithography. *Adv. Mater.* **19**, 4297-4302, (2007).
25. Mizuno, H., Kaneko, T., Sakata, I., Matsubara, K. Capturing by self-assembled block copolymer thin films: transfer printing of metal nanostructures on textured surfaces. *Chem. Commun.* **50**, 362-364, (2014).
26. Mizuno, H., Sai, H., Matsubara, K., Takato, H., Kondo, M. Transfer-printed silver nanodisks for plasmonic light trapping in hydrogenated microcrystalline silicon solar cells. *Appl. Phys. Express.* **7**, 112302-1-4, (2014).
27. Odom, T. W., Love, J. C., Wolfe, D. B., Paul, K. E., Whitesides, G. M. Improved Pattern Transfer in Soft Lithography Using Composite Stamps. *Langmuir* **18**, 5314-5320, (2002).
28. Schmid, H., Michel, B. Siloxane Polymers for High-Resolution, High-Accuracy Soft Lithography. *Macromolecules* **33**, 3042-3049, (2000).
29. Loo, Y.-L., Willett, R. L., Baldwin, K. W., Rogers, J. A. Interfacial Chemistries for Nanoscale Transfer Printing. *J. Am. Chem. Soc.* **124**, 7654-7655, (2002).
30. Hylton, N. P., et al., Loss mitigation in plasmonic solar cells: aluminium nanoparticles for broadband photocurrent enhancements in GaAs photodiodes. *Sci. Rep.* **3**, 2874-1-6, (2013).
31. Delamarche, E., et al., Microcontact Printing Using Poly(dimethylsiloxane) Stamps Hydrophilized by Poly(ethylene oxide) Silanes. *Langmuir* **19**, 8749-8758, (2003).
32. Mizuno, H., Sai, H., Matsubara, K., Kondo, M. Plasmonic Light Trapping in Amorphous Si Solar Cells Using Periodic Ag Nanodisk Structures. *MRS Proc.* **1627**, mrsf13-1627-I05-03, (2014).